Volume 1 | Number 1 | Jan 2013 | Pages 1–100

Analyst

www.rsc.org/analyst

ROYAL SOCIETY OF CHEMISTRY

www.rsc.org/analyst

Detection of Trace Heavy Metal Ions in Water by Nanostructured Porous Si Biosensors

Giorgi Shtenberg[1], Naama Massad-Ivanir[2] and Ester Segal[2,3]*

[1]The Inter-Departmental Program of Biotechnology, [2]Department of Biotechnology and Food Engineering, [3]The Russell Berrie Nanotechnology Institute, Technion – Israel Institute of Technology, Haifa 32000, Israel

Corresponding Author

*E-mail: esegal@tx.technion.ac.il; phone: +972-4-8295071

Abstract

A generic biosensing platform, based on nanostructured porous Si (PSi), Fabry-Pérot thin films, for label-free monitoring of heavy metal ions in aqueous solutions by enzymatic activity inhibition, is described. First, we show a general detection assay by immobilizing horseradish peroxidase (HRP) within the oxidized PSi nanostructure and monitor its catalytic activity in real-time by reflective interferometric Fourier transform spectroscopy. Optical studies reveal high specificity and sensitivity of the HRP-immobilized PSi towards three metal ions (Ag^+>Pb^{2+}>Cu^{2+}), with a detection limit range of 60-120 ppb. Next, we demonstrate the concept of specific detection of Cu^{2+} ions (as a model heavy metal) by immobilizing Laccase, a multi-copper oxidase, within the oxidized PSi. The resulting biosensor allows for specific detection and quantification of copper ions in real water samples by monitoring the Laccase relative

activity. The optical biosensing results are found to be in excellent agreement with those obtained by the gold standard analytical technique (ICP-AES) for all water samples. The main advantage of the presented biosensing concept is the ability to detect heavy metal ions, at environmentally relevant concentrations, using a simple and portable experimental setup, while the specific biosensor design can be tailored by varying the enzyme type.

Keywords Heavy Metals, Optical Biosensors, Porous Si, Enzyme, Laccase, Horseradish Peroxidase

1. Introduction

Heavy metals are one of the most serious environmental pollution problems of our time, threatening global sustainability as being non-biodegradable [1, 2]. Increasing industrial activity and the use of metallic constituents of pesticides leads to the accumulation of heavy metals in the food chain [3]. Lead, chromium, cadmium, copper, zinc, arsenic, and mercury are highly toxic even in trace level (damage or reduce mental and central nervous functions, affect blood composition, lungs, kidneys, liver, and other vital organs) [1, 4]. Long-term exposure may result in severe neurological degenerative conditions, cancer, and in extreme cases may lead to death [5]. Consequently, growing environmental awareness has resulted in strict regulations for reducing heavy metals presence in the environment [6-8]. Therefore, rapid and reliable monitoring of heavy metals in the environment (soil, water resources), drinking water and food, is essential [9]. Traditional quantitative methods for heavy metals analysis include: cold vapor atomic absorption spectroscopy, inductively coupled plasma – mass spectroscopy, inductively coupled plasma – atomic emission spectroscopy, UV-VIS spectroscopy, anodic stripping voltammetry and X-ray absorption spectroscopy [10-13]. These laboratory-based techniques are highly selective and

sensitive (as low as part per-trillion concentrations) [1, 14], but require tedious sample preparation and pre-concentration procedures, involve time-consuming and laborious procedures that can be carried out only by trained professionals, as well as the use of expensive and complex instrumentation [7, 15]. In contrast, biosensors have demonstrated a great potential to exceed these limitations in terms of ease of detection, portability, high-throughput analysis of several pollutants and miniaturization toward lab-on-chip technology, while leveraging and even improving sensitivity (10^{-9}-10^{-20} M) and selectivity [1, 3, 6, 7, 14, 16-24]. To date, a variety of enzymes have been used for heavy metal analysis based on enzymatic inhibition [1, 3, 6, 25-28]. Nomngongo *et al*. have designed an amperometric biosensor for the determination of selected heavy metals based on peroxidase inhibition [11]. The enzyme is immobilized on a platinum-polyaniline electrode, while real water samples are analyzed. The resulting biosensor exhibits a fast response and high sensitivity (limit of detection of 0.091, 0.033 and 0.1 ppb for cadmium, lead and copper, respectively) in correlation to standard analytical techniques. In another study, a whole-cell is immobilized onto a solid support, while the enzymatic activity of alkaline phosphatase is monitored by an optical fiber [29]. The enzyme remains in its natural surrounding resulting in a long-term stability and reflects high sensitivity for toxic inhibition.

Nanostructured porous Si (PSi) has been recognized as versatile platform for numerous sensing and biosensing applications, mainly for its tunable optical properties and large surface area [30-33]. PSi-based interferometers, are highly sensitive to the presence of chemical or biological molecules within the pores, due to the change in the average refractive index of the nanostructure [34-36]. Ultimately, the porous scaffold offers an unbiased label-free optical detection of a wide variety of biomolecular interactions, e.g., enzyme-substrate [37-42], antibody-antigen [43, 44] and DNA fragments [45-47], which are facilitated over small working area [48-50].

In the present work we have designed and fabricated a simple optical biosensing platform based on PSi nanostructures that allows for real-time monitoring of heavy metal ions by enzymatic activity inhibition. Specific interaction of heavy metal ions with the target enzyme, which is immobilized onto the pore walls, modulates a noticeable reduction in the enzymatic activity. This immediately translates into a shift in the reflectivity spectrum of the PSi film, owing to the change in its effective optical thickness (EOT). The present study demonstrates the inhibition sensing concept for horseradish peroxidase (HRP), which is one of the most active peroxidases and often used as a powerful tool in biotechnology [37, 51]. Once, a general detection scheme of heavy metal ions in real water samples at environmentally relevant concentrations is established, using HRP-immobilized PSi, a specific assay is designed to allow detection and quantification of a single metal ion i.e., copper ions. Thus, the PSi platform is modified with a specific enzyme, Laccase, for selective identification and quantification of the copper ions in the complex water samples. The resulting proof-of-concept offers a simple, cost effective, reliable analysis of heavy metals onsite (e.g., in the field) without the need for additional pretreatments or complex instrumentation.

2. Experimental

2.1. Materials

Silicon wafers (highly-doped p-type, 0.8 mΩ-cm resistivity, ‹100› oriented, Boron-doped) are supplied by Siltronix Corp. Aqueous HF (48%) and ethanol absolute are obtained by Merck. 3-Aminopropyl(triethoxyl)silane (APTES), diisopropylethylamine (DIEA), Bis (N-succinimidyl)carbonate (DSC), Horseradish peroxidase (HRP) type VI, Laccase from *Trametes versicolor*, acetonitrile, hydrogen peroxide (H_2O_2), 1-naphthol, 4-chloro-1-naphthol (4CN), Ampliflu red, ethylenediaminetetraacetic acid (EDTA), heavy metal standards, ions and

analytical grade buffers, phosphate buffered saline (PBS) and HEPES, are supplied by Sigma Aldrich. Water samples (drain and irrigation, pH 6.5, used for blackberries plantation at "El Bosque" in Lucena Del Puerto, Huelva, Spain) were generously supplied by RESFOOD project, supported by the 7th Framework Programme of the European Commission. Tap water samples were collected from the laboratory tap (Technion).

2.2. Preparation of PSi optical transducers

Porous Si Fabry-Pérot thin films are prepared by electrochemical anodization of highly-doped p-type Si at a constant current density, as previously described by Massad-Ivanir *et al.* [35]. Subsequently, the resulting PSi films are thermally oxidized at a temperature of 800°C to yield a porous SiO_2 ($PSiO_2$) layers [52].

2.3. Biofunctionalization of oxidized PSi

The thermally oxidized nanostructures are amino-modified by APTES and DIEA, to activate the surface for DSC grafting, in accordance to Massad-Ivanir *et al.* [35]. The homobifunctional cross-linker is acknowledged for its high reactivity with primary amines [35]. Then, the enzymes (HRP and Laccase) are immobilized onto the $PSiO_2$ surface by reaction between surface Lys groups on the enzymes exterior and the second reactive group of the DSC. The DSC-modified surfaces are incubated with 5 μL of enzyme solution (22.7 μM HRP or 14.3 μM EDTA-treated Laccase) in 0.1 M HEPES buffer (pH 8) for 1 hr. Subsequently, the surfaces are thoroughly washed with HEPES buffer to exclude any un-bounded enzymes from the $PSiO_2$. Note: Laccase solution (100 μM) in HEPES buffer is mixed with 0.3 M EDTA in HEPES for 1 hr, for copper removal from the enzyme center. The resulting, non-active enzyme mixture is purified and concentrated by ultrafiltration (Centricon 30, Millipore). Enzyme concentration is determined spectrophotometrically.

2.4. Infrared Spectroscopy

The modified $PSiO_2$ nanostructures are characterized by attenuated total reflectance Fourier transform infrared (ATR-FTIR) spectroscopy as specified by Massad-Ivanir *et al.* [35].

2.5. HRP enzymatic assay

The enzymatic activity of HRP-modified $PSiO_2$ nanostructures is examined by spectrophotometric analysis, as previously described [33].

2.6. Optical Measurements

Interferometric reflectance spectra of $PSiO_2$ samples are collected using an OceanOptics CCD USB 4000 spectrometer fitted with a microscope objective lens coupled to a bifurcated fiber optic cable. A tungsten light source is focused onto the center of the sample surface with a spot size approx. 1-2 mm^2. Reflectivity data are recorded in the wavelength range of 400-1000 nm, with a spectral acquisition time of 100 ms. Both, illumination of the surface and detection of the reflected light are performed along an axis coincident with the surface normal. All the optical experiments are conducted in a fixed cell in order to assure that the samples reflectivity is measured at the same spot during all the measurements. Spectra are collected using a CCD spectrometer and analyzed by applying fast Fourier transform (FFT), as previously described [43, 53]. Concisely, the EOT refers to the *2nL* term in the Fabry-Pérot formula (where *n* is the average refractive index and *L* is the thickness of the porous film) [53]. The data is presented as the relative EOT and defined as:

$$EOT/EOT_0 = \frac{EOT_{Chemical\,modification}}{EOT_{PSiO_2}}$$ (1)

where $EOT_{Chemical\,modification}$ is the value of *nL* after each biofunctionalization step (e.g., APTES, DSC, enzyme immobilization) and EOT_{PSiO2} is the *nL* value of the neat $PSiO_2$. Note: The

custom-made flow-cell is constructed from two Plexiglas plates, where inlet and outlet ports are drilled in the upper plate. The biosensor is placed in between the plates an O-ring is carefully positioned on it. Four screws are used to tighten the plates and fluids are introduced into the cell using Teflon connectors and tubing [48].

2.7. Optical biosensing of enzymatic activity

HRP activity: HRP-modified $PSiO_2$ nanostructures are washed with HEPES buffer for 20 min. Then, 0.8 mM of 4CN in HEPES buffer is injected and cycled through the flow cell for 20 min, followed HRP activation by the addition of 0.16 M H_2O_2.

Metal ions detection: Enzyme-immobilized surfaces are incubated with an appropriate volume of the metal ion stock solution (Pb^{2+}, Ag^+ and Cu^{2+}) for 40 min before conducting the specific activity tests. Control experiments with other cation stock solutions (i.e., Mg^{2+}, Zn^{2+}, Ca^{2+}, Fe^{2+}, Na^+, K^+) are conducted similarly. The data is presented as inhibition values and defined as:

$$Inhibition\,(\%) = \left(1 - \frac{1-\left(\frac{EOT_{metal}}{EOT_0}\right)_t}{1-\left(\frac{EOT_{no-metal}}{EOT_0}\right)_t}\right) \times 100 \qquad (2)$$

where $\frac{EOT_{metal}}{EOT_0}$ is the value of the relative *nL* after exposure to metal-ions; $\frac{EOT_{no-metal}}{EOT_0}$ is the relative *nL* value with no metal-ions exposure; and *t* refers to the time of the optical reading. The detection limits are calculated from the calibration plots by $3S_a/m$, where S_a is the standard of deviation and *m* is the slope of the linear portion.

Analysis of heavy metal ions in real water samples: Tap, drain and irrigation water samples are first filtered with 0.45 µm pore size membrane filter (to remove residual particles), followed by pH adjustment (pH 7) before conducting the optical analysis. Enzyme-immobilized $PSiO_2$ surfaces are incubated with 50 µL of the unknown water sample for 40 min before conducting the specific activity assays.

Laccase activity assay: Laccase-modified PSiO$_2$ surfaces are washed with 0.1 M PBS buffer solution (pH 6.8) for 20 min. For Laccase activation, 0.8 mM of 1-naphthol in PBS buffer is injected and cycled through the flow cell. Metal detection in standard solutions and real water samples is carried out as aforementioned. The data is presented as the relative activity and defined as:

$$Rel.\,Activity\;(\%) = \left(\frac{1 - \left(\frac{EOT_{metal}}{EOT_0}\right)_t}{1 - \left(\frac{EOT_{no-metal}}{EOT_0}\right)_t} \right) \times 100 \qquad (3)$$

where $\frac{EOT_{metal}}{EOT_0}$ is the value of relative *nL* after metal-ions exposure; $\frac{EOT_{no-metal}}{EOT_0}$ is the value of the relative *nL* with no exposure to metal-ions on the native Laccase (without copper removal); and *t* refers to the time of the optical reading. The reflectivity spectra are recorded every 30 s [37].

2.8. Inductively coupled plasma atomic emission spectroscopy (ICP-AES)

Analysis of water samples (tap, drain and irrigation) is performed using a Varian Vista-Pro ICP-AES by monitoring the atomic emission of Pb^{2+}, Ag^{+} and Cu^{2+} ions.

3. Results and Discussion

3.1. Biosensors design

Porous Si Fabry-Pérot films are prepared by electrochemical anodization, followed by thermal oxidation in air at 800°C to increase stability and hydrophilicity of the nanostructured Si scaffolds [32, 35]. The structural properties of the oxidized nanostructures correspond to previously described data by Segal *et al.* [53]. The porous film is 6,830±150 nm thick and 80±20 nm cylindrical pores. Next, a synthetic approach for immobilizing enzymes (HRP and Laccase) onto

the porous nanostructures is based on a well-studied silanization approach [54]. The different

synthetic steps followed for enzyme immobilization onto the porous scaffold are confirmed by

attenuated total reflectance Fourier transform infrared (ATR-FTIR) spectroscopy and reflective

interferometric Fourier transform spectroscopy (RIFTS), see Fig. S1 and S2 (in the Supporting

Information section), respectively.

### 3.2. Optical detection of heavy metals by enzymatic activity

To assess the enzymatic activity of the anchored enzymes we used RIFTS, which is highly

sensitive to minute changes in the average refractive index of the porous nanostructure. The

overall biosensing concept is illustrated in Scheme 1. Reactions carried out in the enzyme-

immobilized nanostructure by introducing various substrate/inhibitor combinations are

monitored in real-time by acquisition of reflectivity spectra from the porous layer [32, 33]; the

Fourier transform (i.e., EOT value) provides a direct measure of the amount of the enzymatic

reaction products infiltrated into the porous scaffold [37]. Therefore, exposure to an aqueous

solution, containing heavy metal ions, is expected to result in a decreased enzymatic activity [55],

and accordingly a smaller EOT change, see Scheme 1a. Whereas, for enzyme-immobilized

PSiO$_2$ exposed to solutions, with no heavy metal ions, the enzymatic reaction products

accumulate within the nanostructure, inducing a profound shift in the EOT (Scheme 1b).
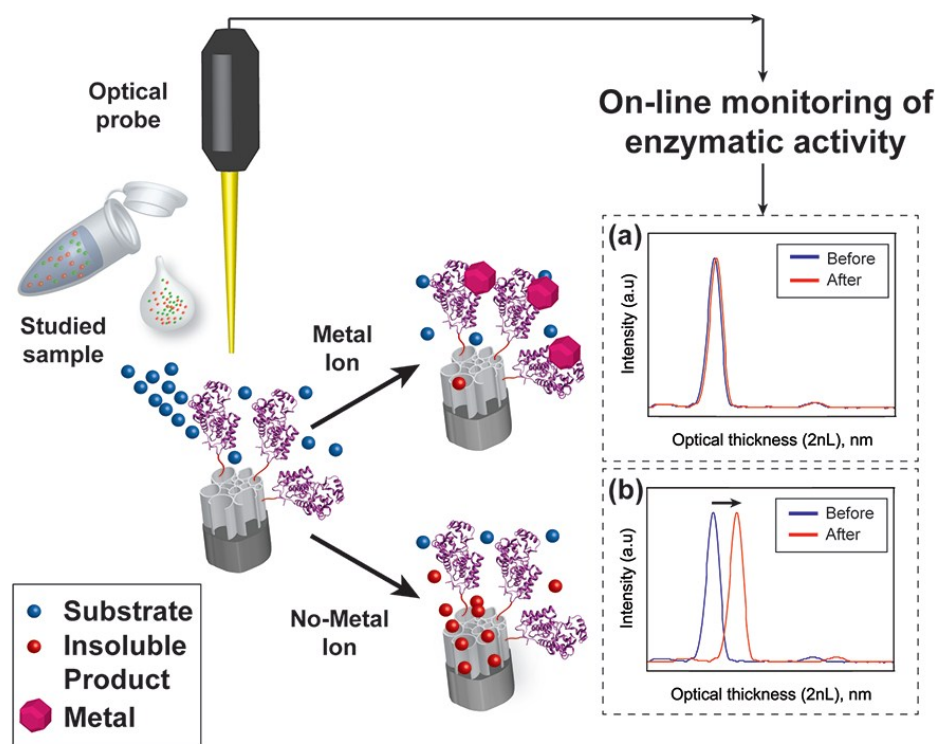
Scheme 1. A schematic illustration of the PSiO$_2$-based optical biosensor for the detection of heavy metals. A minute sample of unknown aqueous solution is incubated with enzyme-functionalized PSiO$_2$, while on-line optical monitoring of enzymatic reaction products is acquired using a simple CCD spectrometer setup. The optical readout correlates to the presence of heavy metal ions in the sample: (a) enzymatic activity inhibition results in a small product quantity infiltrating the PSiO$_2$ scaffold, and insignificant EOT change, whereas (b) the absence of heavy metal ions, present a substantial redshift in the EOT, owing to the accumulation of the insoluble products within the pores.

Figure 1 depicts the relative EOT changes of the HRP-immobilized PSiO$_2$ following exposure to standard aqueous solutions, having different silver ion (Ag$^+$) concentrations. The biosensor is fixed in a custom-made flow cell and incubated with the respective solution for 40 min. It should

10

be noted, complete inhibition of the immobilized HRP by the heavy metal ions occurs after 40 min, as confirmed by specific enzymatic assay (see Fig. S3 in the Supporting Information section). Subsequently, the substrate solution (4CN) is cycled through the flow cell and the optical data acquisition starts after addition of H_2O_2 to the cycled solution. Control experiment with no metal-ions exhibits the highest increase (5.2%) in the relative EOT value. This increase is attributed to the substrate (4CN) oxidation in the presence of the HRP enzyme [37, 56]. The enzymatic reaction products, 4-chloro-1-naphthon, precipitate and accumulate within the pores (as illustrated in Scheme 1b), resulting in a rapid increase in the EOT values with time. Increasing the Ag^+ concentration causes a profound decrease in the relative EOT signal; for a 60 μM Ag^+ solution, a minor increase of less than 0.3% in the relative EOT value is observed (Fig. 1). This behavior is ascribed to the disrupted function of the HRP, which is induced by Ag^+ ions binding to the immobilized enzymes, while causing conformational changes [11, 28].
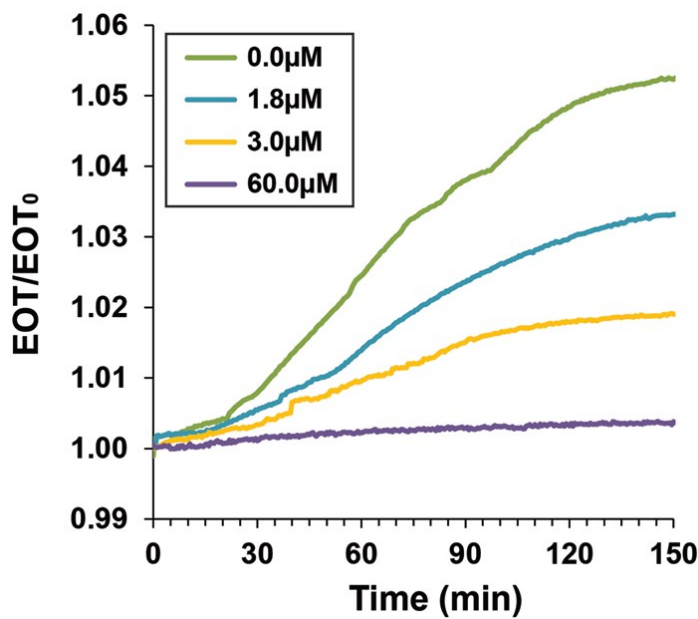
**Fig. 1.** Optical response of HRP-immobilized $PSiO_2$ to different silver ions concentrations. The HRP-modified $PSiO_2$ is incubated with different standard silver ion solutions, followed by

continuous cycling of 0.8 mM 4-chloro-1-naphthol (4CN) in HEPES buffer (pH 8) through the

flow cell. The optical data acquisition starts after addition of H_2O_2 to the cycled solution. The

biosensor is fixed in a custom-made flow cell and the reflectivity spectra are recorded every 30 s.

Next, the selectivity of HRP-immobilized $PSiO_2$ towards different heavy metal ions is studied.

The biosensors are exposed to a wide range of metal ion solutions (at a fixed concentration of 6

µM) and their enzymatic activity is monitored thereafter. Figure 2a summarizes the results of

these experiments and presents the maximal inhibition values (after exposure of 150 min to the

metal ion solution). Significant HRP inhibition is observed after exposure to Ag^+, Pb^{2+} and Cu^{2+}

ions (60%, 49% and 38%, respectively), whereas exposure of the biosensor to other metal ions

i.e., Mg^{2+}, Zn^{2+}, Ca^{2+}, Fe^{2+}, Na^+, and K^+, results in minor inhibition values (<4%). To further

assert these results, possible cumulative effect of these abundant metal ions on the performance

of the biosensor is studied by its exposure to mixtures of metal ions (containing Mg^{2+}, Zn^{2+},

Ca^{2+}, Fe^{2+}, Na^+, K^+, and the different metal ions). Yet, similar inhibition values are obtained (see

Fig. S4), revealing the high selectivity of the biosensor towards the studied heavy metal ions.

These results are assigned to the non-competitive binding of the Ag^+, Pb^{2+} and Cu^{2+} ions to the

enzyme, resulting in conformational changes in its active site, which disrupt and inhibit the HRP

specific activity [11, 26, 57]. The selective behavior of the immobilized HRP is schematically

illustrated in Fig. 2a (inset), depicting the specific interaction of certain metal ions (i.e., Ag^+,

Pb^{2+} and Cu^{2+}) with the enzyme active site while hindering its function. Based on recent studies

[11, 28], the enzymatic activity of HRP is also inhibited by other heavy metal ions including, Cd^{2+},

Co^+, Mn^{2+}, Ni^+ and Hg^{2+} ions. To further demonstrate the selectivity of the biosensor towards the

different metal ions, we have studied the inhibition of the immobilized HRP by different

concentrations of Ag^+, Pb^{2+} and Cu^{2+} ions, in the range of 0.6-100 μM. Figure 2b depicts the

maximal inhibition of the HRP-based biosensor to the three metal ions versus their

concentration. The trend observed in Fig. 2b is consistent with that of Fig. 2a ($Ag^+>Pb^{2+}>Cu^{2+}$).

Additionally, these results are consistent with previous studies [1, 58-60], in which exposure to Ag^+

is observed to exhibit the highest inhibition. The measured detection limit values presented by

HRP-based biosensor are 0.53, 0.60 and 1.63 μM for Ag^+, Pb^{2+} and Cu^{2+}, respectively, or

corresponding to 56, 125 and 104 ppb. While there are more sensitive biosensor designs [1, 7, 8, 26],

the current system detects metal ions in a range that is relevant for environmental monitoring and

real-life application of these biosensors. For example, according to Environmental Protection

Agency (EPA) the maximum copper level in drinking water below which there is no risk to

human health is defined at 1300 ppb [61]. EPA also recommends secondary standards for silver

ions in drinking water not to exceed the level of 100 ppb, in order to prevent undesirable

physiological effects.
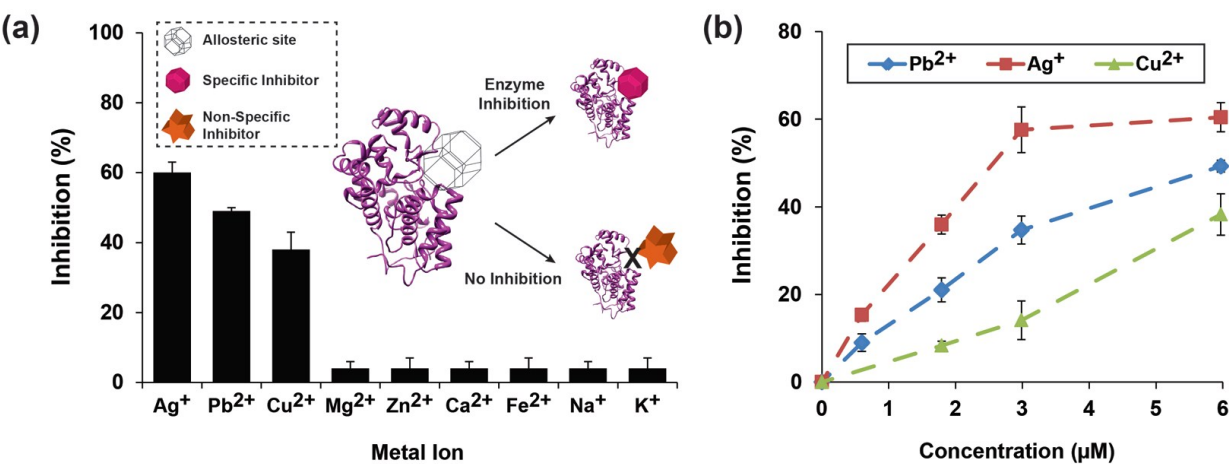
Fig. 2. The inhibition of HRP-immobilized $PSiO_2$ biosensor by: (a) Different metal ions at a

constant concentration (6 μM). Inset: A schematic illustration of the enzymatic inhibition caused

by heavy metals, revealing the selectivity of HRP binding site toward heavy metal ions.

Whereas, regular metal ions are inadequate to HRP binding site. (b) Pb^{2+}, Ag^+ and Cu^{2+} at different concentrations. Data are reported as mean ± standard deviation (n≥4).

3.3. Detection of heavy metals in real water

Once the selectivity and the specificity of our biosensor towards metal pollutants is demonstrated, we investigate the potential of this platform to detect trace levels of heavy metal ions in complex water samples. Thus, HRP-immobilized $PSiO_2$ is exposed to various surface water samples (collected from irrigation and drain sources), while the inhibition values are attained in real time acquisition of the reflectivity spectra. Table 1 depicts the concentration of Ag^+, Pb^{2+} and Cu^{2+} found in tap, drain and irrigation water samples, which are analyzed by both the HRP-based biosensor and the gold standard method of ICP-AES. For drain and irrigation water samples, inhibition values of 9.2±1.4% and 11.3±2.4%, respectively, are obtained. Whereas for tap water, used as a control, less than 3% of HRP inhibition value is attained. These results are in agreement with the ICP-AES analysis, in which only copper ions are detected in drain and irrigation samples (1.4±0.2 and 1.9±0.1 µM, respectively). The ICP-AES results for the tap water show negligible values of the three analyzed metal ions (<0.3 µM). Based on ICP-AES determination of the heavy metal species, we can apply these results in order to quantify the specific metal ion concentration in the studied samples (based on the calibration curves presented in Fig. 2b). Thus, the inhibition values obtained (Table 1) correlate to concentrations of 1.9±0.3 and 2.4±0.5 µM of Cu^{2+} in drain and irrigation water, respectively. These results clearly demonstrate that our biosensing platform can detect the presence of heavy metals in real water samples in relevant concentrations and in agreement with the results of conventional laboratory-

based analytical techniques (i.e., ICP-AES). As such, the main advantages of the presented system are its simplicity and cost efficiency. The HRP-immobilized PSiO$_2$ biosensors can be readily prepared at low cost and high reproducibility, and as detection scheme does not rely on an expensive instrumentation, the developed system might by suitable for in-field applications [21].

3.4. Specific detection and quantification of copper ions

Next, the generic design of the biosensor is altered for specific optical detection and quantification of Cu^{2+}. We use Laccase, which is a multi-copper oxidase, that catalyzes the oxidation of a wide variety of organic and inorganic substrates [62, 63]. It is known for different Laccases, that type II copper can be selectively depleted from the enzyme center and easily reconstructed back [64, 65]. Our concept is to remove the copper from the enzyme prior to its conjugation to the PSiO$_2$ nanostructure. We expect that exposure of the Laccase-immobilized PSiO$_2$ to aqueous samples, containing Cu^{2+}, will induce the reconstruction of the enzyme as the copper ions are embedded into the enzyme center (see Fig. S5). This in turn, will restore the enzyme function, while the extent of this process is optically monitored as the enzymatic reaction products infiltrate into the porous nanostructure. Thus, prior to its immobilization, the Laccase is pretreated with 0.3 M EDTA in HEPES buffer (pH 8) to remove type 2 copper for absolute enzyme inactivation, confirmed by specific activity assay (Fig. S5). Following Laccase immobilization, the resulting biosensor is exposed to different metal ion solutions (at a fixed concentration of 6 μM), while the substrate solution (1-naphthol) is continuously cycled through the flow cell. The optical data acquisition starts immediately after substrate addition to the cycled solution and the relative activity is monitored. Similarly to HRP enzymatic reaction, 1-naphthol is oxidized in the presence of Laccase into insoluble product [66], which precipitate and accumulate within the pores, resulting in a rapid increase in the EOT values with time. The

results of these experiments are summarized in Fig. 3a, which presents the maximal relative activity values (after exposure of 150 min to the metal ion solution) of the Laccase-based biosensor. Upon exposure to Cu^{2+}, a relative activity value of 77% is attained, while exposure to the other screened metal ions results in relative activity values of <8%. In addition, possible cumulative effect of these ions on the performance of the biosensor is also studied by exposure to mixtures of these metal ions. Nonetheless, similar relative activity values are observed (see Fig. S4). Thus, these results demonstrate the specificity of the Laccase-based biosensor towards copper ions, as schematically illustrated in Fig. 3a (inset), while other metal ions have a minor effect on the enzyme activity. Furthermore, the specificity of Laccase-immobilized $PSiO_2$ towards Cu^{2+} ions is further verified by monitoring the relative activity of the enzyme for other heavy metal ions i.e., Ag^{+} and Pb^{2+}, at different concentrations (Fig. 3b). The Laccase-based biosensor exhibits a linear response towards copper ions in the studied concentration range (1.2-6 µM), as opposed its negligible response to Ag^{+} and Pb^{2+} ions. These results confirm the strong affinity between copper ions and the Laccase [66]. The biosensor presents lower detection limit than the HRP-based biosensor (1.30 and 1.63 µM, respectively), revealing the sensitivity of this approach for detecting copper ions in real water samples.
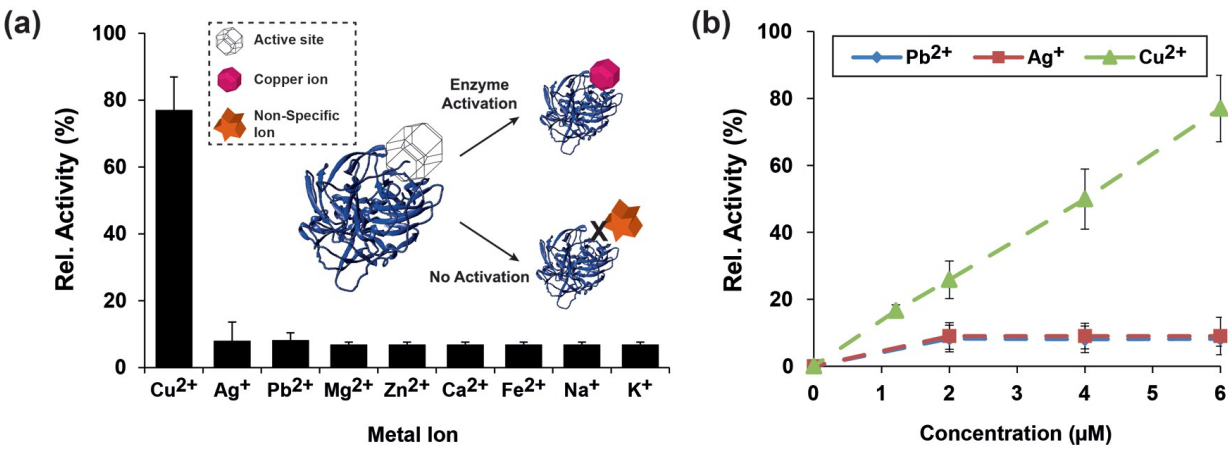
Fig. 3. The relative activity of Laccase-immobilized $PSiO_2$ biosensor by: (a) Different metal ions at a constant concentration (6 μM). Inset: A schematic illustration of the specificity of Laccase toward copper ions, as only copper can bind onto the enzymes active site. (b) Pb^{2+}, Ag^+ and Cu^{2+} at different concentrations. Data are reported as mean $\pm$ standard deviation (n$\geq$4).

Finally, the Laccase-based biosensor is exposed to the "real" water samples as aforementioned, as the relative activity values are attained in real time acquisition of the reflectivity spectra. Table 1 depicts the quantification of Ag^+, Pb^{2+} and Cu^{2+} in tap, drain and irrigation water samples by the Laccase-immobilized $PSiO_2$ biosensor. Drain and irrigation water are found to reactivate the enzyme by 18.5$\pm$1.4% and 24.4$\pm$7.0%, respectively, indicating the presence of copper ions in these samples. Based on the calibration curve presented in Fig. 3b, the obtained relative activity values correlate to Cu^{2+} concentrations of 1.4$\pm$0.1 and 1.9$\pm$0.5 μM (drain and irrigation water, respectively). These results are in excellent agreement with the ICP-AES results presented in Table 1. Cu^{2+} concentration in tap water is found to be negligible, as previously determined by the HRP-based biosensor. Comparison of the laccase-immobilized $PSiO_2$ biosensor to other label-free optical biosensing schemes for detection of copper ions e.g., surface Plasmon resonance [67], shows similar sensitivity (below 100 ppb). Yet, our system is highly specific to

17

copper and employs a simple and inexpensive setup, in comparison to the SPR-based biosensor [67, 68], making it suitable for point-of-care applications.

Table 1. Detection and quantification of real water samples by HRP and Laccase-based optical biosensor and by ICP-AES.

Water sample	HRP optical biosensor		Laccase optical biosensor		ICP-AES		
	Inhibition (%)	Cu^{2+} $(\mu M)^{*}$	Rel. Activity (%)	Cu^{2+} $(\mu M)^{**}$	Ag^{+} (μM)	Pb^{2+} (μM)	Cu^{2+} (μM)
Tap	<3	<0.3	<8	<0.6	<0.3	<0.3	<0.3
Drain	9.2±1.4	1.9±0.3	18.5±1.4	1.4±0.1	<0.3	<0.3	1.4±0.2
Irrigation	11.3±2.4	2.4±0.5	24.4±7.0	1.9±0.5	<0.3	<0.3	1.9±0.1

[*] Calculated based on calibration curve Fig. 2b.
[**] Calculated based on calibration curve Fig. 3b.
Data are reported as mean ± standard deviation (n≥4).

4. Conclusions

An optical biosensing platform is designed for label-free detection and quantification of heavy metals in real surface water samples using a simple and portable experimental setup. We exploit the specificity of specific enzymes to heavy metal ions and hence monitor the catalytic activity in real-time by RIFTS technique. First, we show a general detection assay by immobilizing HRP within the $PSiO_2$ thin film, revealing high sensitivity towards three metal ions ($Ag^{+} > Pb^{2+} > Cu^{2+}$). Next, we demonstrate the concept of specific heavy metal ion detection for Cu^{2+}, by immobilizing Laccase within the $PSiO_2$ scaffold. Using the Laccase-based biosensor we are able to detect the presence of trace levels of Cu^{2+} in real water samples, with values identical to those

obtained by ICP-AES. The generic design of this biosensor will potentially allow tailoring unlimited experimental setups (by varying the model enzymes) for systematic analysis of heavy metal pollutants in aqueous surroundings. Nevertheless, these enzyme-based biosensors should be further optimized in terms their stability, reusability, specificity and shelf life prior to their implementation in the field.

Supporting Information

ATR-FTIR spectra, relative EOT of the different functionalization steps and the relative enzymatic activity vs. incubation time. This material is available free of charge via the Internet at http://pubs.acs.org.

Acknowledgment

References

1. N. Verma and M. Singh, *Biometals*, 2005, **18**, 121-129.
2. M. S. Moorthy, H.-J. Cho, E.-J. Yu, Y.-S. Jung and C.-S. Ha, *Chem. Commun.*, 2013, **49**, 8758-8760.
3. N. Tekaya, O. Saiapina, H. Ben Ouada, F. Lagarde, H. Ben Ouada and N. Jaffrezic-Renault, *Bioelectrochemistry*, 2013, **90**, 24-29.
4. X. Liu, Q. Song, Y. Tang, W. Li, J. Xu, J. Wu, F. Wang and P. C. Brookes, *Sci. Total Environ.*, 2013, **463–464**, 530-540.
5. S. A. Al Bakheet, I. M. Attafi, Z. H. Maayah, A. R. Abd-Allah, Y. A. Asiri and H. M. Korashy, *Environ. Pollut.*, 2013, **181**, 226-232.
6. A. Samphao, H. Rerkchai, J. Jitcharoen, D. Nacapricha and K. Kalcher, *Int. J. Electrochem. Sci.*, 2012, **7**, 1001-1010.
7. M. Li, H. Gou, I. Al-Ogaidi and N. Wu, *ACS Sustainable Chem. Eng.*, 2013, **1**, 713-723.

8.   M. Benounis, N. Jaffrezic-Renault, H. Halouani, R. Lamartine and I. Dumazet-Bonnamour, *Mater. Sci. Eng., C*, 2006, **26**, 364-368.

9.   A. M. López Marzo, J. Pons, D. A. Blake and A. Merkoçi, *Biosens. Bioelectron.*, 2013, **47**, 190-198.

10.   J. Morton, N. Havens, A. Mugweru and A. K. Wanekaya, *Electroanalysis*, 2009, **21**, 1597-1603.

11.   N. Nomngongo, C. Ngilia and T. Msagati, in *Biosensors - Emerging Materials and Applications*, ed. P. A. Serra, InTech, 2011, ch. 25, pp. 569-588.

12.   W. Yue, B. L. Riehl, N. Pantelic, K. T. Schlueter, J. M. Johnson, R. A. Wilson, X. Guo, E. E. King and W. R. Heineman, *Electroanalysis*, 2012, **24**, 1039-1046.

13.   D. Zhao, X. Guo, T. Wang, N. Alvarez, V. N. Shanov and W. R. Heineman, *Electroanalysis*, 2014, **26**, 488-496.

14.   P. D. Selid, H. Xu, E. M. Collins, M. S. Face-Collins and J. X. Zhao, *Sensors*, 2009, **9**, 5446-5459.

15.   D. T. Quang and J. S. Kim, *Chem. Rev.*, 2010, **110**, 6280-6301.

16.   F. Long, A. Zhu, C. Gu and H. Shi, in *State of the Art in Biosensors - Environmental and Medical Applications*, ed. T. Rinken, InTech, Croatia, 2013, ch. 1, pp. 3-28.

17.   Z. Zhang, A. Tang, S. Liao, P. Chen, Z. Wu, G. Shen and R. Yu, *Biosens. Bioelectron.*, 2011, **26**, 3320-3324.

18.   T. Kumeria, A. Santos and D. Losic, *ACS Appl. Mater. Interfaces*, 2013, **5**, 11783-11790.

19.   F. Long, A. Zhu, H. Shi, H. Wang and J. Liu, *Sci. Rep.*, 2013, DOI: 10.1038/srep02308.

20.   A. Eshkeiti, B. B. Narakathu, A. S. G. Reddy, A. Moorthi, M. Z. Atashbar, E. Rebrosova, M. Rebros and M. Joyce, *Sens. Actuators, B*, 2012, **171**, 705-711.

21.   G. Aragay, J. Pons and A. Merkoçi, *Chem. Rev.*, 2011, **111**, 3433-3458.

22.   L. Wang, T. Li, Y. Du, C. Chen, B. Li, M. Zhou and S. Dong, *Biosens. Bioelectron.*, 2010, **25**, 2622-2626.

23.   H. Zhang, L. Yang, B. Zhou, W. Liu, J. Ge, J. Wu, Y. Wang and P. Wang, *Biosens. Bioelectron.*, 2013, **47**, 391-395.

24.   Y. Xiao, A. A. Rowe and K. W. Plaxco, *J. Am. Chem. Soc.*, 2006, **129**, 262-263.

25.   B. B. Rodriguez, J. A. Bolbot and I. E. Tothill, *Biosens. Bioelectron.*, 2004, **19**, 1157-1167.

26.   A. Amine, H. Mohammadi, I. Bourais and G. Palleschi, *Biosens. Bioelectron.*, 2006, **21**, 1405-1423.

27.   H. Tsai and R. Doong, *Biosens. Bioelectron.*, 2005, **20**, 1796-1804.

28.   B. Silwana, C. Van der Horst, E. Iwuoha and V. Somerset, in *State of the Art in Biosensors - Environmental and Medical Applications*, ed. R. Toonika, InTech, 2013, vol. 5, pp. 105-119.

29.   C. Durrieu and C. Tran-Minh, *Ecotoxicol. Environ. Saf.*, 2002, **51**, 206-209.

30.   A. Jane, R. Dronov, A. Hodges and N. H. Voelcker, *Trends Biotechnol.*, 2009, **27**, 230-239.

31.   M. J. Sailor and J. R. Link, *Chem. Commun.*, 2005, **11**, 1375-1383.

32.   M. M. Orosco, C. Pacholski and M. J. Sailor, *Nat. Nanotechnol.*, 2009, **4**, 255-258.

33.   G. Shtenberg, N. Massad-Ivanir, O. Moscovitz, S. Engin, M. Sharon, L. Fruk and E. Segal, *Anal. Chem.*, 2013, **85**, 1951-1956.

34.   P. D'Orazio, *Clin. Chim. Acta*, 2003, **334**, 41-69.

35. N. Massad-Ivanir, G. Shtenberg, A. Tzur, M. A. Krepker and E. Segal, *Anal. Chem.*, 2011, **83**, 3282-3289.
36. K. A. Kilian, T. Bocking and J. J. Gooding, *Chem. Commun.*, 2009, 630-640.
37. G. Shtenberg, N. Massad-Ivanir, S. Engin, M. Sharon, L. Fruk and E. Segal, *Nanoscale Res. Lett.*, 2012, **7**, 1-6.
38. Y. Shang, W. Zhao, E. Xu, C. Tong and J. Wu, *Biosens. Bioelectron.*, 2010, **25**, 1056-1063.
39. H. Qiao, B. Guan, J. J. Gooding and P. J. Reece, *Opt. Express*, 2010, **18**, 15174-15182.
40. J. Shang, F. Cheng, M. Dubey, J. M. Kaplan, M. Rawal, X. Jiang, D. S. Newburg, P. A. Sullivan, R. B. Andrade and D. M. Ratner, *Langmuir*, 2012, **28**, 3338-3344.
41. L. A. DeLouise, P. M. Kou and B. L. Miller, *Anal. Chem.*, 2005, **77**, 3222-3230.
42. M. A. Krepker and E. Segal, *Anal. Chem.*, 2013, **85**, 7353-7360.
43. N. Massad-Ivanir, G. Shtenberg, T. Zeidman and E. Segal, *Adv. Funct. Mater.*, 2010, **20**, 2269-2277.
44. N. Massad-Ivanir, G. Shtenberg and E. Segal, *Adv. Exp. Med. Biol.*, 2012, **733**, 37-45.
45. L. De Stefano, P. Arcari, A. Lamberti, C. Sanges, L. Rotiroti, I. Rea and I. Rendina, *Sensors*, 2007, **7**, 214-221.
46. I. Rea, A. Lamberti, I. Rendina, G. Coppola, M. Gioffre, M. Iodice, M. Casalino, E. De Tommasi and L. De Stefano, *J. Appl. Phys.*, 2010, **107**.
47. G. Rong, A. Najmaie, J. E. Sipe and S. M. Weiss, *Biosens. Bioelectron.*, 2008, **23**, 1572-1576.
48. L. M. Bonanno and E. Segal, *Nanomedicine*, 2011, **6**, 1755-1770.
49. K. A. Kilian, T. Böcking, K. Gaus, M. Gal and J. J. Gooding, *ACS Nano*, 2007, **1**, 355-361.
50. A. H. Soeriyadi, B. Gupta, P. J. Reece and J. J. Gooding, *Polym. Chem.*, 2014, **5**, 2333-2341.
51. A. M. Azevedo, V. C. Martins, D. M. Prazeres, V. Vojinovic, J. M. Cabral and L. P. Fonseca, *Biotechnol. Annu. Rev.*, 2003, **9**, 199-247.
52. G. Shtenberg, N. Massad-Ivanir, L. Fruk and E. Segal, *ACS Appl. Mater. Interfaces*, 2014, **6**, 16049–16055.
53. E. Segal, L. A. Perelman, F. Cunin, F. Di Renzo, J. M. Devoisselle, Y. Y. Li and M. J. Sailor, *Adv. Funct. Mater.*, 2007, **17**, 1153-1162.
54. B. Xia, S. J. Xiao, D. J. Guo, J. Wang, M. Chao, H. B. Liu, J. Pei, Y. Q. Chen, Y. C. Tang and J. N. Liu, *J. Mater. Chem.*, 2006, **16**, 570-578.
55. A. Y. Louie and T. J. Meade, *Chem. Rev.*, 1999, **99**, 2711-2734.
56. F. Patolsky, M. Zayats, E. Katz and I. Willner, *Anal. Chem.*, 1999, **71**, 3171-3180.
57. C. Chen, Q. Xie, L. Wang, C. Qin, F. Xie, S. Yao and J. Chen, *Anal. Chem.*, 2011, **83**, 2660-2666.
58. J. C. Gayet, A. Haouz, A. Geloso-Meyer and C. Burstein, *Biosens. Bioelectron.*, 1993, **8**, 177-183.
59. A. P. Soldatkin, V. Volotovsky, A. V. El'skaya, N. Jaffrezic-Renault and C. Martelet, *Anal. Chim. Acta*, 2000, **403**, 25-29.
60. C. Preininger and O. S. Wolfbeis, *Biosens. Bioelectron.*, 1996, **11**, 981-990.
61. L. H. Nowell and E. A. Resek, *Rev. Environ. Contam. Toxicol.*, 1994, **140**, 1-164.
62. C. F. Thurston, *Microbiology*, 1994, **140**, 19-26.

63. O. V. Morozova, G. P. Shumakovich, M. A. Gorbacheva, S. V. Shleev and A. L. Yaropolov, *Biochemistry*, 2007, **72**, 1136-1150.
64. C. Bukh and M. J. Bjerrum, *J. Inorg. Biochem.*, 2010, **104**, 1029-1037.
65. V. Madhavi and S. S. Lele, *Bioresources*, 2009, **4**, 1694-1717.
66. J. Kulys, R. Vidziunaite and P. Schneider, *Enzyme Microb. Technol.*, 2003, **32**, 455-463.
67. R. Wang, W. Wang, H. Ren and J. Chae, *Biosens. Bioelectron.*, 2014, **57**, 179-185.
68. R. Verma and B. D. Gupta, *Food Chem.*, 2015, **166**, 568-575.